JACS
JOURNAL OF THE AMERICAN CHEMICAL SOCIETY
Article
pubs.acs.org/JACS

Tuning the Adsorption-Induced Phase Change in the Flexible Metal–Organic Framework Co(bdp)

Mercedes K. Taylor,[†,§] Tomče Runčevski,[†,§] Julia Oktawiec,[†] Miguel I. Gonzalez,[†] Rebecca L. Siegelman,[†] Jarad A. Mason,[†,§] Jinxing Ye,[∥] Craig M. Brown,[⊥,#] and Jeffrey R. Long*[,†,‡,§]

[†]Department of Chemistry and [‡]Department of Chemical and Biomolecular Engineering, University of California, Berkeley, California 94720, United States

[§]Materials Sciences Division, Lawrence Berkeley National Laboratory, Berkeley, California 94720, United States

[∥]Engineering Research Center of Pharmaceutical Process Chemistry, Ministry of Education; School of Pharmacy, East China University of Science and Technology, 130 Meilong Road, Shanghai 200237, China

[⊥]NIST Center for Neutron Research, National Institute of Standards and Technology, Gaithersburg, Maryland 20899, United States

[#]Department of Chemical and Biomolecular Engineering, University of Delaware, Newark, Delaware 19716, United States

Supporting Information

ABSTRACT: Metal–organic frameworks that flex to undergo structural phase changes upon gas adsorption are promising materials for gas storage and separations, and achieving synthetic control over the pressure at which these changes occur is crucial to the design of such materials for specific applications. To this end, a new family of materials based on the flexible metal–organic framework Co(bdp) (bdp^{2-} = 1,4-benzenedipyrazolate) has been prepared via the introduction of fluorine, deuterium, and methyl functional groups on the bdp^{2-} ligand, namely, Co(F-bdp), Co(*p*-F_2-bdp), Co(*o*-F_2-bdp), Co(D_4-bdp), and Co(*p*-Me_2-bdp). These frameworks are isoreticular to the parent framework and exhibit similar structural flexibility, transitioning from a low-porosity, collapsed phase to high-porosity, expanded phases with increasing gas pressure. Powder X-ray diffraction studies reveal that fluorination of the aryl ring disrupts edge-to-face π–π interactions, which work to stabilize the collapsed phase at low gas pressures, while deuteration preserves these interactions and methylation strengthens them. In agreement with these observations, high-pressure CH_4 adsorption isotherms show that the pressure of the CH_4-induced framework expansion can be systematically controlled by ligand functionalization, as materials without edge-to-face interactions in the collapsed phase expand at lower CH_4 pressures, while frameworks with strengthened edge-to-face interactions expand at higher pressures. Importantly, this work puts forth a general design strategy relevant to many other families of flexible metal–organic frameworks, which will be a powerful tool in optimizing these phase-change materials for industrial applications.

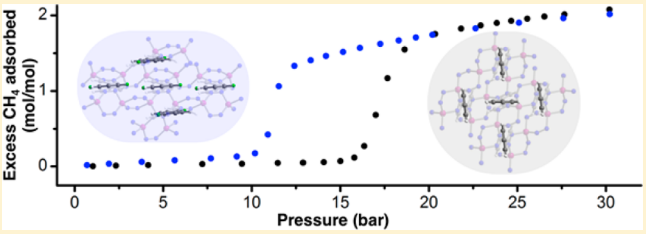

INTRODUCTION

Metal–organic frameworks are a unique class of three-dimensional materials composed of metal ions linked by multitopic organic ligands, which are notable for their crystallinity, porosity, and synthetic tunability.[1] Certain metal–organic frameworks also demonstrate structural flexibility, reversibly responding to external stimuli, such as changes in temperature or gas pressure.[2] Flexible frameworks that collapse under reduced gas pressure and expand under increasing pressure are particularly promising for gas storage applications, because of the unique shape of their adsorption isotherms. These materials adsorb minimal gas below the phase change pressure and then exhibit an abrupt rise or "step" in adsorption upon undergoing the phase change. This drastic change in adsorption behavior can lead to enhanced selectivities, high usable storage capacities, and reduced thermal management requirements.[3] A handful of recent studies have found that, particularly in the case of the metal–organic framework MIL-53, changing the ligand functionality alters the step pressure.[4] In general, for a given family of flexible metal–organic frameworks, identification of the structural features that give rise to the phase change should allow the pressure at which this step occurs in the adsorption isotherm to be tuned through chemical design.

A promising system for such a structure–property relationship study is the flexible metal–organic framework Co(bdp) (bdp^{2-} = 1,4-benzenedipyrazolate).[2f,l] This material features a record-high usable capacity for methane storage due to a sharp step at 18 bar in its high-pressure (0–70 bar) CH_4 adsorption isotherm, which results from a structural transition from a collapsed phase to an expanded phase under increasing gas pressure. This expansion is also endothermic, endowing the framework with the ability to provide intrinsic thermal

Received: August 31, 2016

DOI: 10.1021/jacs.6b09155
J. Am. Chem. Soc. XXXX, XXX, XXX–XXX

management.[3e] However, potential gains in CH_4 thermal management and usable capacity are only realized if the operating pressure range for a given application spans the spread of the isotherm step. For example, many CH_4 sources emit CH_4 at pressures well below 18 bar, including low-pressure natural gas formations and biogas generation facilities.[5] To achieve on-site CH_4 storage or transport to processing facilities without costly initial compression would require an adsorbent for which the phase change occurs at lower pressures than that of Co(bdp). Alternatively, for the material to be suitable for storage of a more weakly interacting gas such as hydrogen,[6] or a more strongly interacting gas such as carbon dioxide,[7] the adsorption step position must be shifted accordingly. Therefore, the ability to tune the phase change pressure of a flexible adsorbent like Co(bdp) through synthesis is vital to the industrial application of these materials.

In the collapsed phase of Co(bdp), edge-to-face $\pi-\pi$ interactions between the aryl rings of neighboring bdp^{2-} ligands likely contribute to the stability of the collapsed phase at low gas pressures and affect the energy required to expand the framework.[3e,8] We hypothesized that introduction of different functional groups on the central ring of bdp^{2-} would alter the strength of these interactions and therefore alter the minimum CH_4 pressure necessary to produce the isotherm step. In particular, we anticipated that increasing the strength of the edge-to-face interactions would lead to higher step pressures, while decreasing their strength would lead to lower step pressures.

Herein, we demonstrate control over the phase change pressure via systematic ligand modification in a new series of functionalized Co(bdp) frameworks. X-ray diffraction studies and low-pressure N_2 adsorption measurements indicate that all new derivatives are isoreticular to Co(bdp) and exhibit similar structural flexibility. To study the effects of ligand functionalization, CH_4 was used as a probe molecule for high-pressure adsorption measurements and in situ powder X-ray diffraction experiments, allowing us to rationalize changes in step pressures relative to the nonfunctionalized framework. Because the operating conditions for industrial gas adsorption applications vary widely, this ability to systematically tune the position of an isotherm step is of tremendous advantage in facilitating the design of new adsorbents. Moreover, the synthetic approach outlined here can likely be applied to other flexible metal−organic frameworks and gases, enabling materials scientists to design phase-change adsorbents for specific applications.

EXPERIMENTAL SECTION

Unless otherwise stated, all manipulations were performed under an Ar or N_2 atmosphere in a Vacuum Atmospheres glovebox or using standard Schlenk techniques. Anhydrous *N*,*N*-dimethylformamide (DMF) and anhydrous dichloromethane (CH_2Cl_2) were obtained from a JC Meyer solvent system. All other reagents were obtained from commercial vendors and used as received.

Synthesis of H_2bdp Derivatives. The ligand 1,4-benzenedipyrazole (H_2bdp) was synthesized according to a previously reported procedure.[2f] Complete synthetic details and characterization for all other functionalized H_2bdp derivatives are provided in the Supporting Information, while a general procedure is given below. The functionalized dibromobenzene analogues used were 1,4-dibromo-2-fluorobenzene, 1,4-dibromo-2,5-difluorobenzene, 1,4-dibromo-2,3-difluorobenzene, 1,4-dibromobenzene-d_4, or 1,4-dibromo-2,5-dimethylbenzene.

Functionalized 1,4-dibromobenzene (8.00 mmol, 1.00 equiv), 1-(2-tetrahydropyranyl)-1*H*-pyrazole-4-boronic acid pinacol ester (5.56 g, 20.0 mmol, 2.50 equiv), and K_3PO_4 (8.48 g, 40.0 mmol, 5.00 equiv) were suspended in toluene (16 mL) in a 40 mL glass scintillation vial equipped with a magnetic stir bar, which was then sparged with Ar for 10 min. The vial was uncapped quickly to add XPhos Pd G2[9] (1.26 g, 1.60 mmol, 0.200 equiv) and then briefly purged with Ar, sealed with a PTFE-lined cap, and heated to 110 °C with stirring for 2 days. After 2 days, the reaction mixture was cooled to room temperature, exposed to air, concentrated under reduced pressure, and diluted with 250 mL of diethyl ether. The ether layer was then washed with saturated aqueous $NaHCO_3$ (5 × 250 mL), dried over $MgSO_4$, and concentrated under reduced pressure to yield a yellow oil, which was used in the subsequent reaction without additional purification. The crude ligand was then dissolved in 60 mL of methanol in a 250 mL round-bottom flask equipped with a magnetic stir bar. To this flask was added 12 mL of concentrated aqueous HCl, and the reaction mixture was stirred at 50 °C for 2 h, during which time a white precipitate formed. The reaction mixture was then filtered, and the filtrate was suspended in water and neutralized with $NaHCO_3$. The precipitate was isolated in a second filtration, washed with water, and dried under reduced pressure to yield a white or beige powder.

Synthesis of Co(bdp) Derivatives. The compound Co(bdp) and all Co(bdp) derivatives were synthesized using a strategy adapted from a previous report.[2f] Specifically, a 100 mL solvent bomb was charged with a magnetic stir bar, $Co(CF_3SO_3)_2$ (0.72 g, 2.0 mmol, 1.1 equiv), H_2bdp or H_2bdp derivative (1.9 mmol, 1.0 equiv), and 10 mL of *N*,*N*-diethylformamide (DEF). The mixture was degassed using five freeze−pump−thaw cycles and then sealed by closing the stopcock of the solvent bomb while the frozen reaction mixture remained under vacuum. The solvent bomb was then heated at 160 °C for 3 days to afford a purple microcrystalline solid. Upon completion of the reaction, the solvent bomb was backfilled with Ar, the supernatant was removed under positive Ar pressure and discarded, and 80 mL of anhydrous DMF was added to the solid product under an Ar atmosphere. The solvent bomb was then sealed under Ar and heated to 110 °C overnight. This solvent-exchange procedure was performed once daily for 7 days to completely remove unreacted starting material from the pores. Subsequently, the DMF was replaced with anhydrous CH_2Cl_2 following the same procedure but without heating. These CH_2Cl_2 exchanges were performed once daily for 3 days to allow activation from a lower-boiling solvent. To activate the material, the CH_2Cl_2 was evaporated under positive Ar pressure until 25 mL of solution remained. The resultant slurry was transferred to a 100 mL Schlenk flask under inert atmosphere, and the CH_2Cl_2 was evaporated over the course of 1 h under a flow of Ar at room temperature. The resultant solid was dried under a flow of Ar at 160 °C for 6 h and then placed under dynamic vacuum at 160 °C overnight. The activated solid was immediately transferred to a glovebox and handled under a dinitrogen atmosphere for all further experiments.

Single-Crystal and Powder X-ray Diffraction. All single-crystal X-ray diffraction data were collected at Beamline 11.3.1 at the Advanced Light Source, Lawrence Berkeley National Laboratory, using synchrotron radiation (λ = 0.7749 Å for Co(bdp), Co(D_4-bdp), and Co(F-bdp); λ = 0.8856 for Co(*o*-F_2-bdp) and Co(*p*-F_2-bdp)) with a Bruker PHOTON100 CMOS detector on a D8 diffractometer. The samples were held at the experimental temperature under N_2 using an Oxford Cryosystems cryostream during data collection.

High-resolution powder X-ray diffraction patterns of the samples were collected at the Beamline 17-BM at the Advanced Photon Source of Argonne National Laboratory with an average wavelength of 0.72768 Å. Scattered intensity was recorded by a PerkinElmer α-Si Flat Panel detector. Prior to measurement, the samples were packed in borosilicate glass capillaries of 1 mm diameter (Hilgenberg glass No. 50) under a N_2 atmosphere, and the capillaries were then attached to a gas-dosing manifold for in situ diffraction measurements. For each sample, diffraction patterns were collected at room temperature under dynamic vacuum to obtain the structure of the material in the collapsed phase. For Co(*p*-F_2-bdp), the gas-dosing manifold was then used to increase CH_4 pressure in increments of approximately 3 bar

DOI: 10.1021/jacs.6b09155
J. Am. Chem. Soc. XXXX, XXX, XXX−XXX

from 0 to 19.7 bar, and diffraction data for each pressure was collected after reaching equilibrium (evidenced by a constant pressure readout and diffraction pattern). Analysis of all diffraction data, including structure solution and refinement, is discussed in the Supporting Information.

Gas Adsorption. Nitrogen adsorption isotherms for pressures in the range of 0−1.1 bar were measured using a Micromeritics ASAP 2020 or 2420 gas adsorption analyzer. Activated samples were transferred under a N_2 atmosphere to preweighed analysis tubes, which were capped with a Transeal. Each sample was evacuated on the instrument until the outgas rate was less than 3 μbar/min. The evacuated analysis tube containing degassed sample was then carefully transferred to an electronic balance and weighed to determine the mass of sample (typically 30−50 mg). The tube was then fitted with an isothermal jacket and transferred back to the analysis port of the instrument. The outgas rate was again confirmed to be less than 3 μbar/min. Nitrogen adsorption isotherms were measured at 77 K using a liquid N_2 bath.

Methane adsorption isotherms for pressures in the range of 0−70 bar were measured on an HPVA-II-100 gas adsorption analyzer from Particulate Systems, a Micromeritics company. In a typical measurement, 0.2−0.5 g of activated sample was loaded into a tared stainless steel sample holder inside a glovebox under a N_2 atmosphere. Prior to connecting the sample holder to the VCR fittings of the complete high-pressure assembly inside the glovebox, the sample holder was weighed to determine the sample mass. The sample holder was then transferred to the HPVA-II-100, connected to the analysis port of the instrument via an OCR fitting, and evacuated at room temperature for at least 2 h. The sample holder was then placed inside an aluminum recirculating dewar connected to a Julabo FP89-HL isothermal bath filled with Julabo Thermal C2 fluid. The temperature stability of the isothermal bath was ±0.02 °C. Methods for accurately measuring the relevant sample freespaces, which involve the expansion of He from a calibrated volume at 0.7 bar and 25 °C to the evacuated sample holder, have been described in detail previously.[18l] Nonideality corrections were performed using the CH_4 compressibility factors tabulated in the NIST REFPROP database[10] at each measured temperature and pressure.

RESULTS AND DISCUSSION

Synthesis of Functionalized Co(bdp) Derivatives. Variants of the H_2bdp ligand with methyl, deuterium, or fluorine functionalities on the central ring were synthesized to investigate how changing the noncovalent interactions between linkers in the collapsed Co(bdp) phase might influence adsorption-induced structural changes. Specifically, the selected groups were expected to show increased, similar, or decreased electrostatic affinities for the π cloud of a neighboring aryl ring, respectively.[8,11,12] This array of dipyrazole ligands was realized by coupling protected pyrazoleboronic esters to a variety of commercially available dibromobenzenes (Scheme 1), thus enabling late-stage diversification. Initial attempts to accomplish this coupling with $Pd(PPh_3)_4$ required large amounts of the catalyst, high reaction temperatures, and long reaction times, and still resulted in low yields and incomplete conversions. This inefficiency was especially true of the multiply fluorinated substrates; for example, the synthesis of H_2(*o*-F_2-bdp) required the gradual addition of 0.6 equiv of $Pd(PPh_3)_4$ over the course of 8 days of heating at reflux. In turn, the liberal use of $Pd(PPh_3)_4$ led to an abundance of PPh_3O byproduct, which was difficult to remove completely from the desired product via chromatography. In order to improve the syntheses and minimize impurities carried forward, we optimized the coupling reaction conditions through a series of trials and ultimately adopted XPhos Pd G2[9] as a catalyst in place of $Pd(PPh_3)_4$. Although a minimum of 0.2 equiv of catalyst was still necessary

Scheme 1. Synthesis of H_2bdp Derivatives

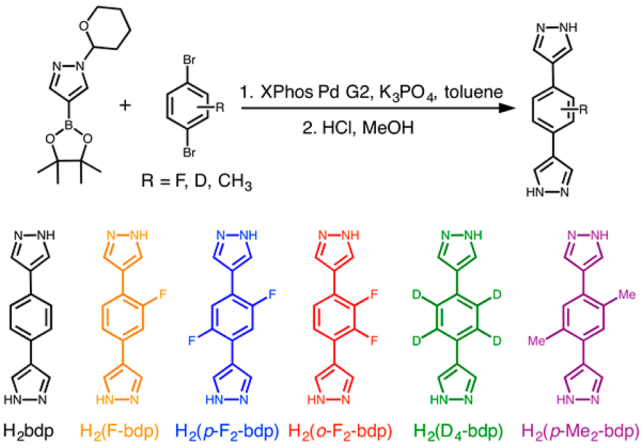

for the synthesis of the fluorinated H_2bdp derivatives, this route afforded improved yields and reduced reaction times (see the Supporting Information for full experimental details).

The corresponding Co(bdp) derivatives were synthesized by reaction of $Co(CF_3SO_3)_2$ with the respective ligands in sealed vessels with *N*,*N*-diethylformamide (DEF), and after heating at 160 °C for 3 days, the desired frameworks were obtained as dark purple crystalline solids. It was found that in comparison to the parent framework, the fluorinated derivatives are much more air-sensitive. Framework degradation was evidenced by formation of pink, red, or brown solids that were shown to be amorphous by powder X-ray diffraction. In addition to this color change and loss of crystallinity, prestep adsorption in subsequent CH_4 adsorption isotherms was often a sign that a material was of insufficient quality (Figure S20). Sample degradation occurred frequently during postsynthetic solvent exchanges in particular, and this degradation was ultimately overcome by carrying out all exchanges using anhydrous solvent and rigorous Schlenk techniques, precautions that are unnecessary for Co(bdp). We also note that fluorination of H_2bdp reduces the solubility of the ligand in DMF, and thus more extensive solvent exchanges are necessary to remove unreacted materials from the pores of the resulting metal−organic framework.

After optimization of the synthesis conditions for all Co(bdp) derivatives, crystals suitable for single-crystal X-ray diffraction were obtained for Co(F-bdp), Co(*p*-F_2-bdp), Co(*o*-F_2-bdp), and Co(D_4-bdp) from small-scale reactions in sealed tubes. The resultant DEF-solvated crystal structures confirmed the formation of metal−organic frameworks with the same structural connectivity as Co(bdp). The as-synthesized materials adopt an expanded configuration, in which one-dimensional square channels are formed by chains of tetrahedral pyrazolate-bridged cobalt(II) centers linked on four sides by rows of bdp^{2-} ligands. As an example, a portion of the structure of the solvated Co(*p*-F_2-bdp) is depicted in Figure 1. Interestingly, the fluorinated aryl rings in this structure are ordered, such that fluorine atoms from one ring are oriented toward fluorine atoms on adjacent rings along the walls of the channel. The resulting C−F···F−C distance between adjacent ligands is 2.693(6) Å, slightly shorter than the mean C−F···F−C distance of 2.8 Å found in a survey of the CSD for aromatic C−F···F−C contacts below the sum of the van der Waals radii.[13] Thus, the overall framework geometry positions the rings at a distance compatible with typical C−F···F−C

DOI: 10.1021/jacs.6b09155
J. Am. Chem. Soc. XXXX, XXX, XXX−XXX

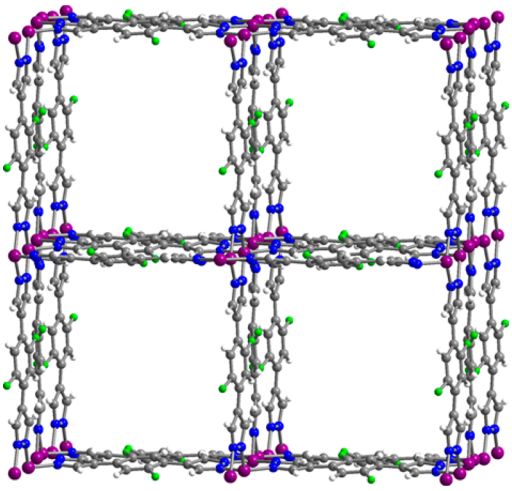

Figure 1. Single-crystal X-ray diffraction structure of DEF-solvated form of Co(p-F_2-bdp). DEF molecules in the framework pores were found to be disordered and could not be modeled successfully and thus are not shown here. All Co(bdp) derivatives feature one-dimensional channels bounded by rows of organic ligands and chains of tetrahedral cobalt(II) ions. Gray, blue, white, purple, and green spheres represent C, N, H, Co, and F atoms, respectively.

interactions and gives rise to aryl ordering in Co(p-F_2-bdp),[14] as discussed further below. Single crystals of Co(bdp) were also obtained, and improved resolution data and a better structural refinement were achieved relative to the original report[2f] by collecting data at room temperature. Although a single-crystal structure determination was not obtained for Co(p-Me_2-bdp), its structure was confirmed to be isoreticular to that of Co(bdp) from powder X-ray diffraction data collected for the activated bulk sample (Figure S6).

N_2 Adsorption and Framework Flexibility. Prior to gas adsorption measurements, all frameworks were activated by heating the materials to 160 °C under dynamic vacuum to completely remove any guest solvent molecules. Low-temperature N_2 adsorption measurements were then used to assess the porosity and flexibility of the various derivatives (Figure 2). Similar to the N_2 isotherm of Co(bdp), the new frameworks

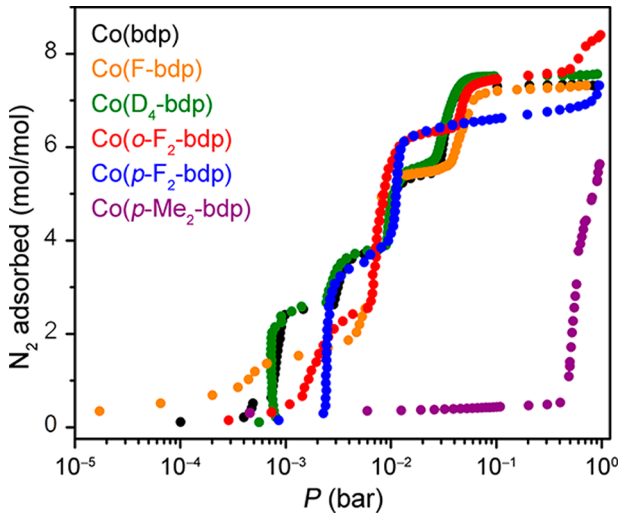

Figure 2. Low pressure N_2 adsorption for Co(bdp) and derivatives at 77 K. Co(bdp) adsorption (black) largely underlays Co(D_4-bdp) adsorption (green).

Co(F-bdp), Co(p-F_2-bdp), Co(o-F_2-bdp), and Co(D_4-bdp) exhibit low initial N_2 uptake, followed by a series of distinct adsorption steps beginning at pressures below 3 mbar. This isotherm shape indicates that these materials are collapsed when fully evacuated, but transition to a series of expanded structures under increasing gas pressure, demonstrating that the introduction of new functional groups does not eliminate framework flexibility. The step positions in each isotherm vary among the derivatives, suggesting that the stability of each structural intermediate (and thus the N_2 pressure associated with that particular phase change) is uniquely affected by ligand functionalization. All of the aforementioned Co(bdp) derivatives reach an expanded phase with N_2 saturation capacities between 7.1 and 8.3 mol/mol, indicating that these materials have similarly high permanent porosities, with Langmuir surface areas between 2279 and 2702 m^2/g (Table S3). In contrast, Co(p-Me_2-bdp) remains relatively nonporous until nearly 500 mbar, at which point it undergoes a phase change to reach a saturation capacity of only 5.3 mol/mol. This much higher phase change pressure suggests that the ligand methyl groups significantly stabilize a collapsed framework structure.[15]

Structural Characterization of Collapsed Phases. To investigate the effect of ligand functionalization on edge-to-face $\pi-\pi$ interactions in the collapsed phases of these materials, the frameworks Co(D_4-bdp), Co(p-Me_2-bdp), and Co(p-F_2-bdp) were chosen as representatives of each type of functional group, and synchrotron powder X-ray diffraction data were collected on the activated powders while they were maintained under dynamic vacuum at room temperature. As expected, the activated structure of Co(D_4-bdp) does not exhibit noticeable differences from Co(bdp) and adopts a collapsed phase with a calculated pore volume of 0 cm^3/g.[16] While the diffraction data revealed that Co(p-F_2-bdp) and Co(p-Me_2-bdp) also adopt collapsed phases, these structures display important differences from the parent framework (Figure 3).

In the case of Co(p-Me_2-bdp), the ligands interact across the pore channel through edge-to-face $\pi-\pi$ interactions, similar to those of Co(bdp) and Co(D_4-bdp). However, because of the steric bulk of the methyl groups, the methylated aryl rings are not able to orient perpendicularly or approach as closely as the phenyl rings in the parent framework. Indeed, the distance between the centers of two adjacent aryl rings in Co(p-Me_2-bdp) is 5.6 Å, compared to 4.9 Å in Co(bdp). Consequently, Co(p-Me_2-bdp) retains some porosity in its collapsed phase, with a calculated accessible N_2 surface area of 59 m^2/g and pore volume of 0.021 cm^3/g[16] that is consistent with the 77 K N_2 adsorption approaching 1.5 mmol/g prior to any structural changes. Despite this increased porosity, the comparatively high expansion pressure of Co(p-Me_2-bdp) suggests that its collapsed phase is significantly more stable than that of the other Co(bdp) derivatives. This increased stability can be understood by considering the activated, collapsed structure: the methyl group orients two of its three hydrogen atoms toward the neighboring phenyl ring π cloud, increasing the number of electrophilic atoms engaged in the edge-to-face interaction. Furthermore, the electron-donating nature of the methyl group strengthens the edge-to-face interaction by increasing the electron density in the π cloud, as well as the electrophilicity of the edge of the ring.[11]

In Co(p-Me_2-bdp), as well as Co(bdp) and Co(D_4-bdp), the edge-to-face interactions across pore channels are facilitated by a rotation of the ligands relative to the associated chain of cobalt atoms. Alternating ligands rotate either clockwise or

DOI: 10.1021/jacs.6b09155
J. Am. Chem. Soc. XXXX, XXX, XXX−XXX

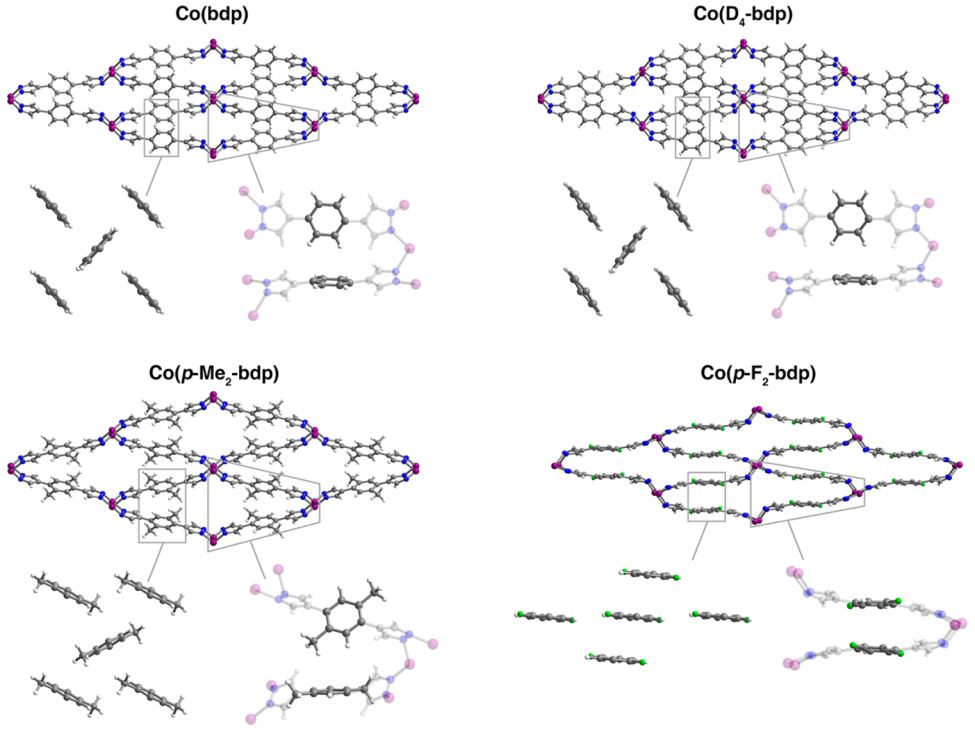

Figure 3. Powder X-ray diffraction structures of activated Co(bdp), Co(D_4-bdp), Co(p-Me_2-bdp), and Co(p-F_2-bdp), viewed down the pore channel. Below each structure are expanded views, highlighting interactions between the aryl rings of the frameworks. Gray, blue, white, purple, and green spheres represent C, N, H, Co, and F atoms, respectively.

counterclockwise, orienting the electron-poor edge of one aryl ring toward the electron-rich π cloud of the next in a stabilizing electrostatic interaction (Figure S10).[8,12] This orientation results in a dihedral angle between successive ligands of as large as 73.7° for Co(bdp). In the case of Co(p-F_2-bdp), however, this dihedral angle is only 9.7°, and edge-to-face interactions are replaced with a π-stacked configuration, wherein the fluorine atoms of one ligand sit above the hydrogen atoms of another. Thus, the introduction of electronegative fluorine atoms onto the central ligand ring in Co(p-F_2-bdp) decreases the electronic disparity between ring edge and face, thereby decreasing the favorability of this edge-to-face interaction.

Methane-Induced Phase Change. To evaluate the effect of ligand variation on adsorption-induced structural changes, CH_4 (the main component of natural gas) was selected as a probe molecule for high-pressure adsorption measurements. In addition to the industrial relevance of natural gas as a heating, electricity, and transportation fuel and to the growing interest in its storage in metal−organic frameworks, CH_4 was chosen as a probe because it is supercritical at ambient temperature, which avoids contributions from pore condensation that might complicate structure−property investigations.[1b,3e,17,18]

High-pressure CH_4 adsorption isotherms were measured for all Co(bdp) derivatives from 1 to 70 bar at 25 °C, revealing that the introduction of various substituents indeed results in shifts in the phase change step pressure (Figures 4 and S21). Importantly, these altered step pressures are consistent with the structural information obtained from diffraction studies. For example, the CH_4 isotherm of Co(D_4-bdp) exhibits minimal low-pressure adsorption followed by a sharp step at ∼18 bar and nearly overlays with the isotherm of Co(bdp). Thus, any equilibrium isotope effect is likely to be small. In stark contrast, the CH_4 adsorption isotherm of Co(p-Me_2-bdp) exhibits no

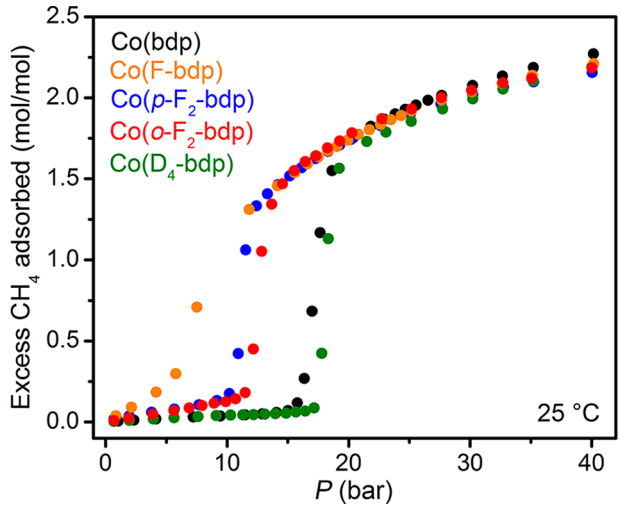

Figure 4. High-pressure CH_4 adsorption isotherms of Co(bdp), Co(F-bdp), Co(p-F_2-bdp), Co(o-F_2-bdp), and Co(D_4-bdp) at 25 °C.

phase change below 70 bar (Figure S22) and instead adopts a Type I shape with modest gas uptake. This behavior is indicative of a slightly porous, rigid material, consistent with the porosity observed for the activated Co(p-Me_2-bdp) structure. Because the low-pressure N_2 adsorption of Co(p-Me_2-bdp) shows that this framework is indeed flexible, we hypothesize that the CH_4-induced phase change occurs at much higher pressures than in Co(bdp), as is the case for the N_2-induced phase change. Again, this result supports the conclusions drawn from the activated structure of Co(p-Me_2-bdp), in which the methyl groups enhance the favorable edge-to-face π−π interactions in the collapsed structure and thus stabilize this phase.

DOI: 10.1021/jacs.6b09155
J. Am. Chem. Soc. XXXX, XXX, XXX−XXX

For Co(F-bdp), Co(p-F_2-bdp), and Co(o-F_2-bdp), on the other hand, the step shifts to lower CH_4 pressures relative to Co(bdp), indicating that the collapsed phase is destabilized by the introduction of fluorine atoms.[15] This observation is consistent with the powder diffraction data for the collapsed phase of Co(p-F_2-bdp), in which the stabilizing edge-to-face $\pi-\pi$ interactions are eliminated. However, in addition to the crystal structure of the collapsed phase, a structure of the CH_4-expanded phase is necessary to fully understand how fluorination affects the step pressure. Therefore, we continued to focus on Co(p-F_2-bdp) as a representative of fluorine functionalization, and in situ diffraction studies at variable CH_4 pressures were performed on this compound.

The in situ diffraction patterns for Co(p-F_2-bdp) show that the step is indeed the result of a discrete structural phase change, in which the material expands by 103% in unit cell volume from 0 to 20 bar, as the calculated pore volume increases from 0 cm^3/g to 0.98 cm^3/g[16] (Figure S). In contrast

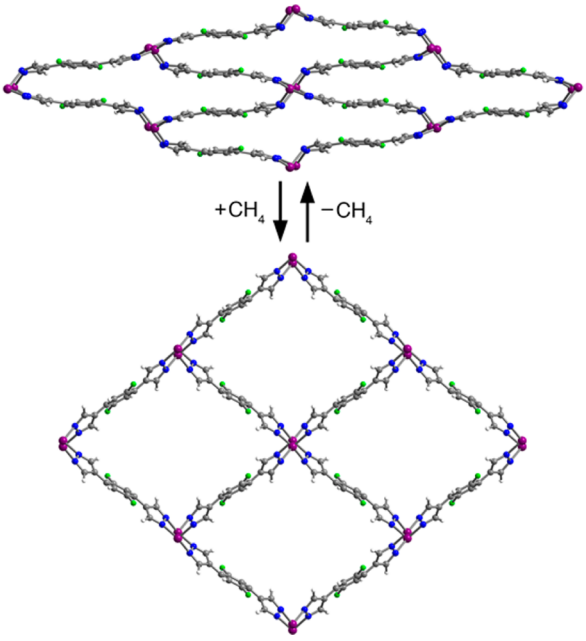

Figure 5. Powder X-ray diffraction structures of Co(p-F_2-bdp) under vacuum (top) and under 20 bar CH_4 (bottom). Gray, blue, white, purple, and green spheres represent C, N, H, Co, and F atoms, respectively.

to the DEF-solvated structure of Co(p-F_2-bdp), in which fluorine atoms on adjacent rings orient toward each other, both the activated and CH_4-expanded structures show the aryl rings to order in the opposite orientation, with fluorine atoms pointing toward adjacent hydrogen atoms (Figure S9). This C−H···F−C interaction has the characteristics of a weak hydrogen bond and has been shown to influence the conformation of other systems containing aryl fluorides.[19] Although it has been shown that C−H···F−C interactions are preferred over C−F···F−C interactions in fluorobenzenes,[20] our results suggest that the carbon−carbon distance may be an important factor in determining which interaction is most favorable. In the collapsed and CH_4-expanded phases of Co(p-F_2-bdp), in which the aryl rings are ordered to achieve C−H···F−C interactions, the relevant carbon atoms are separated by 4.7 and 4.8 Å, respectively. But in the fully expanded, DEF-solvated structure, these carbons are 5.0 Å apart, and the aryl rings are rotated to replace the C−H···F−C interactions with C−F···F−C interactions. We note that this conclusion is not firm, however, since the disordered guest DEF molecules within the channels may also somehow be influencing the aryl ring arrangement.

Because the lateral C−H···F−C interactions are maintained when Co(p-F_2-bdp) undergoes the CH_4-induced phase change, only two $\pi-\pi$ stacking interactions involving the central ring must be broken to accomplish the expansion. This is in distinct contrast to the four edge-to-face $\pi-\pi$ interactions that must be broken in collapsed Co(bdp). Indeed, the reduction in the number of $\pi-\pi$ interactions that must be broken in the CH_4-induced phase change is likely a key factor in the destabilization of collapsed Co(p-F_2-bdp) relative to Co(bdp). The destabilizing effect of fluorination extends to Co(o-F_2-bdp) and Co(F-bdp), which also exhibit phase changes at lower CH_4 pressures than the unfunctionalized framework. However, while both Co(o-F_2-bdp) and Co(p-F_2-bdp) undergo phase changes at ∼11 bar CH_4, Co(F-bdp) expands below 8 bar, indicating that the collapsed phase of the monofluorinated derivative is less stable than that of the difluorinated materials. This result implies that the number of fluorine atoms on the aryl ring, and not their relative location, is the dominant factor influencing the strength of $\pi-\pi$ stacking. We note that this evidence is consistent with earlier observations[21] that substituents strengthen $\pi-\pi$ stacking through local interactions with the opposing ring, rather than through their effect on the net dipole of the aryl system.

CONCLUSIONS

In this work, we used structural insights to design and synthesize a new family of isoreticular metal−organic frameworks derived from the flexible framework Co(bdp). By introducing methyl or fluoro substituents onto the central ring of the ligand, the step in the CH_4 adsorption isotherm of the parent Co(bdp) compound could be shifted to higher or lower pressures, respectively. In situ powder X-ray diffraction studies show that the shifts in the CH_4-induced phase change pressure are due to the enhancement or disruption of key $\pi-\pi$ interactions in the collapsed phase of these materials. The shifts in step pressure correlate with the nature of the substituent in a predictable fashion, facilitating the design of future materials with a desired step pressure in mind. This relationship between ligand structure and phase-change pressure may also be leveraged in other flexible metal−organic frameworks, by using crystal structures of the collapsed and expanded phases to identify interactions that are formed or broken during the phase change. Although we have focused here on the edge-to-face $\pi-\pi$ interactions present in the collapsed phase of Co(bdp), many other noncovalent, intraframework interactions may readily be targeted depending on the metal−organic framework. Once linkers have been identified that modulate the targeted interactions, the step pressure could potentially be further tuned by using a mixture of linkers to synthesize a multivariate metal−organic framework with an intermediate step pressure. Such synthetic control over the phase change pressures of flexible metal−organic frameworks is a powerful and promising tool for their application in an industrial setting.

ASSOCIATED CONTENT

Supporting Information

The Supporting Information is available free of charge on the ACS Publications website at DOI: 10.1021/jacs.6b09155.

DOI: 10.1021/jacs.6b09155
J. Am. Chem. Soc. XXXX, XXX, XXX−XXX

Crystal data for Co(p-F_2-bdp), solvated (CIF)
Crystal data for Co(o-F_2-bdp), solvated (CIF)
Crystal data for Co(F-bdp), solvated (CIF)
Crystal data for Co(D_4-bdp), solvated (CIF)
Crystal data for Co(bdp), solvated (CIF)
Crystal data for Co(Me_2-bdp), collapsed (CIF)
Crystal data for Co(D_4-bdp), collapsed (CIF)
Crystal data for Co(p-F_2-bdp), collapsed (CIF)
Crystal data for Co(p-F_2-bdp), expanded (CIF)
Synthetic details and descriptions of crystallographic and gas adsorption data analysis (PDF)

AUTHOR INFORMATION

Corresponding Author

*jrlong@berkeley.edu

Notes

The authors declare no competing financial interest.

ACKNOWLEDGMENTS

Early stages of the synthetic chemistry, including the synthesis of H_2(F-bdp) and Co(F-bdp), were supported by the U.S. Department of Energy, Advanced Research Projects Agency–Energy (ARPA-e). The remainder of the synthetic chemistry was funded by the Department of Energy, Office of Energy Efficiency and Renewable Energy, Fuel Cell Technologies Office under Grant DE-AC02-05CH11231. Methane adsorption measurements and structural studies were supported by the Center for Gas Separations Relevant to Clean Energy Technologies, an Energy Frontier Research Center supported by the U.S. Department of Energy, Office of Science, Office of Basic Energy Sciences, under Award DE-SC0001015. Single-crystal diffraction data were collected on the 11.3.1 Beamline at the Advanced Light Source User Facility at Lawrence Berkeley National Laboratory, which is supported by the Director, Office of Science, Office of Basic Energy Sciences, of the U.S. Department of Energy. Powder X-ray diffraction data were collected on the 17-BM Beamline at the Advanced Photon Source, a U.S. Department of Energy Office of Science User Facility operated by Argonne National Laboratory. We thank Douglas Reed, Matthew Kapelewski, Dr. Brian Wiers, and Prof. Jiwoong Lee for helpful discussions and for experimental assistance, and Dr. Katie R. Meihaus for editorial assistance. We also thank the National Science Foundation for providing graduate fellowship support for M.K.T., J.O., and J.A.M.

REFERENCES

(1) (a) Li, H.; Eddaoudi, M.; O'Keefe, M.; Yaghi, O. M. *Nature* **1999**, *402*, 276. (b) Eddaoudi, M.; Kim, J.; Rosi, N.; Vodak, D.; Wachter, J.; O'Keeffe, M.; Yaghi, O. M. *Science* **2002**, *295*, 469. (c) Kitagawa, S.; Kitaura, R.; Noro, S.-I. *Angew. Chem., Int. Ed.* **2004**, *43*, 2334. (d) Matsuda, R.; Kitaura, R.; Kitagawa, S.; Kubota, Y.; Belosludov, R. V.; Kobayashi, T. C.; Sakamoto, H.; Chiba, T.; Takata, M.; Kawazoe, Y.; Mita, Y. *Nature* **2005**, *436*, 238. (e) Férey, G. *Chem. Soc. Rev.* **2008**, *37*, 191. (f) Morris, R. E.; Wheatley, P. S. *Angew. Chem., Int. Ed.* **2008**, *47*, 4966. (g) Czaja, A. U.; Trukhan, N.; Müller, U. *Chem. Soc. Rev.* **2009**, *38*, 1284. (h) Li, J.-R.; Kuppler, R. J.; Zhou, H.-C. *Chem. Soc. Rev.* **2009**, *38*, 1477. (i) Chen, B.; Xiang, S.; Qian, G. *Acc. Chem. Res.* **2010**, *43*, 1115. (j) Zhou, H.-C.; Long, J. R.; Yaghi, O. M. *Chem. Rev.* **2012**, *112*, 673. (k) Evans, J. D.; Sumby, C. J.; Doonan, C. J. *Chem. Soc. Rev.* **2014**, *43*, 5933.

(2) (a) Kitagawa, S.; Kondo, M. *Bull. Chem. Soc. Jpn.* **1998**, *71*, 1739. (b) Cussen, E. J.; Claridge, J. B.; Rosseinsky, M. J.; Kepert, C. J. *J. Am. Chem. Soc.* **2002**, *124*, 9574. (c) Llewellyn, P. L.; Bourrelly, S.; Serre, C.; Filinchuk, Y.; Férey, G. *Angew. Chem., Int. Ed.* **2006**, *45*, 7751. (d) Kondo, A.; Noguchi, H.; Carlucci, L.; Proserpio, D. M.; Ciani, G.; Kajiro, H.; Ohba, T.; Kanoh, H.; Kaneko, K. *J. Am. Chem. Soc.* **2007**, *129*, 12362. (e) Serre, C.; Mellot-Draznieks, C.; Surblé, S.; Audebrand, N.; Filinchuk, Y.; Férey, G. *Science* **2007**, *315*, 1828. (f) Choi, H. J.; Dincă, M.; Long, J. R. *J. Am. Chem. Soc.* **2008**, *130*, 7848. (g) Thallapally, P. K.; Tian, J.; Radha Kishan, M.; Fernandez, C. A.; Dalgarno, S. J.; McGrail, P. B.; Warren, J. E.; Atwood, J. L. *J. Am. Chem. Soc.* **2008**, *130*, 16842. (h) Férey, G.; Serre, C. *Chem. Soc. Rev.* **2009**, *38*, 1380. (i) Horike, S.; Shimomura, S.; Kitagawa, S. *Nat. Chem.* **2009**, *1*, 695. (j) Demessence, A.; Long, J. R. *Chem. - Eur. J.* **2010**, *16*, 5902. (k) Fernandez, C. A.; Thallapally, P. K.; Motkuri, R. K.; Nune, S. K.; Sumrak, J. C.; Tian, J.; Liu, J. *Cryst. Growth Des.* **2010**, *10*, 1037. (l) Salles, F.; Maurin, G.; Serre, C.; Llewellyn, P. L.; Knöfel, C.; Choi, H. J.; Filinchuk, Y.; Oliviero, L.; Vimont, A.; Long, J. R.; Férey, G. *J. Am. Chem. Soc.* **2010**, *132*, 13782. (m) Liu, Y.-Y.; Couck, S.; Vandichel, M.; Grzywa, M.; Leus, K.; Biswas, S.; Volkmer, D.; Gascon, J.; Kapteijn, F.; Denayer, J. F. M.; Waroquier, M.; Van Speybroeck, V.; Van Der Voort, P. *Inorg. Chem.* **2013**, *52*, 113. (n) Sato, H.; Kosaka, W.; Matsuda, R.; Hori, A.; Hijikata, Y.; Belosludov, R. V.; Sakaki, S.; Takata, M.; Kitagawa, S. *Science* **2014**, *343*, 167. (o) Schneemann, A.; Bon, V.; Schwedler, I.; Senkovska, I.; Kaskel, S.; Fischer, R. A. *Chem. Soc. Rev.* **2014**, *43*, 6062. (p) Lanza, A.; Germann, L. S.; Fisch, M.; Casati, N.; Macchi, P. *J. Am. Chem. Soc.* **2015**, *137*, 13072. (q) Sadakiyo, M.; Yamada, T.; Kato, K.; Takata, M.; Kitagawa, H. *Chem. Sci.* **2016**, *7*, 1349.

(3) (a) Kitaura, R.; Seki, K.; Akiyama, G.; Kitagawa, S. *Angew. Chem., Int. Ed.* **2003**, *42*, 428. (b) Zhao, X.; Xiao, B.; Fletcher, A. J.; Thomas, K. M.; Bradshaw, D.; Rosseinsky, M. J. *Science* **2004**, *306*, 1012. (c) Noguchi, H.; Kondoh, A.; Hattori, Y.; Kanoh, H.; Kajiro, H.; Kaneko, K. *J. Phys. Chem. B* **2005**, *109*, 13851. (d) Llewellyn, P. L.; Horcajada, P.; Maurin, G.; Devic, T.; Rosenbach, N.; Bourrelly, S.; Serre, C.; Vincent, D.; Loera-Serna, S.; Filinchuk, Y.; Férey, G. *J. Am. Chem. Soc.* **2009**, *131*, 13002. (e) Mason, J. A.; Oktawiec, J.; Taylor, M. K.; Hudson, M. R.; Rodriguez, J.; Bachman, J. E.; Gonzalez, M. I.; Cervellino, A.; Guagliardi, A.; Brown, C. M.; Llewellyn, P. L.; Masciocchi, N.; Long, J. R. *Nature* **2015**, *527*, 357.

(4) (a) Couck, S.; Denayer, J. F. M.; Baron, G. V.; Rémy, T.; Gascon, J.; Kapteijn, F. *J. Am. Chem. Soc.* **2009**, *131*, 6326. (b) Devic, T.; Horcajada, P.; Serre, C.; Salles, F.; Maurin, G.; Moulin, B.; Heurtaux, D.; Clet, G.; Vimont, A.; Grenéche, J.-M.; Le Ouay, B.; Moreau, F.; Magnier, E.; Filinchuk, Y.; Marrot, J.; Lavalley, J.-C.; Daturi, M.; Férey, G. *J. Am. Chem. Soc.* **2010**, *132*, 1127. (c) Horcajada, P.; Salles, F.; Wuttke, S.; Devic, T.; Heurtaux, D.; Maurin, G.; Vimont, A.; Daturi, M.; David, O.; Magnier, E.; Stock, N.; Filinchuk, Y.; Popov, D.; Riekel, C.; Férey, G.; Serre, C. *J. Am. Chem. Soc.* **2011**, *133*, 17839. (d) Ramsahye, N. A.; Trung, T. K.; Bourrelly, S.; Yang, Q.; Devic, T.; Maurin, G.; Horcajada, P.; Llewellyn, P. L.; Yot, P.; Serre, C.; Filinchuk, Y.; Fajula, F.; Férey, G.; Trens, P. *J. Phys. Chem. C* **2011**, *115*, 18683. (e) Henke, S.; Schneemann, A.; Wütscher, A.; Fischer, R. A. *J. Am. Chem. Soc.* **2012**, *134*, 9464. (f) Lescouet, T.; Kockrick, E.; Bergeret, G.; Pera-Titus, M.; Aguado, S.; Farrusseng, D. *J. Mater. Chem.* **2012**, *22*, 10287. (g) Serra-Crespo, P.; Gobechiya, E.; Ramos-Fernandez, E. V.; Juan-Alcañiz, J.; Martinez-Joaristi, A.; Stavitski, E.; Kirschhock, C. E. A.; Martens, J. A.; Kapteijn, F.; Gascon, J. *Langmuir* **2012**, *28*, 12916. (h) Kozachuk, O.; Meilikhov, M.; Yusenko, K.; Schneemann, A.; Jee, B.; Kuttatheyil, A. V.; Bertmer, M.; Sternemann, C.; Pöppl, A.; Fischer, R. A. *Eur. J. Inorg. Chem.* **2013**, *2013*, 4546.

(5) (a) Neumann, H.-J.; Paczynska-Lahme, B. Natural Gas. In *Ullmann's Encyclopedia of Industrial Chemistry*, 5th ed.; Elvers, B., Hawkins, S., Schulz, G., Eds.; VCH: Weinheim, 1991; pp 73–124. (b) Yadvika; Santosh; Sreekrishnan, T. R.; Kohli, S.; Rana, V. *Bioresour. Technol.* **2004**, *95*, 1. (c) Balat, M.; Balat, H. *Energy Sources, Part A* **2009**, *31*, 1280. (d) Kidnay, A. J.; Parrish, W. R.; McCartney, D. G. *Fundamentals of Natural Gas Processing*, 2nd ed.; CRC Press: Boca Raton, FL, 2009. (e) Mazyan, W.; Ahmadi, A.; Ahmed, H.; Hoorfar, M. *J. Nat. Gas Sci. Eng.* **2016**, *30*, 487.

(6) (a) Rowsell, J. L. C.; Millward, A. R.; Park, K. S.; Yaghi, O. M. *J. Am. Chem. Soc.* **2004**, *126*, 5666. (b) Dietzel, P. D. C.; Panella, B.; Hirscher, M.; Blom, R.; Fjellvåg, H. *Chem. Commun.* **2006**, *9*, 959.

DOI: 10.1021/jacs.6b09155
J. Am. Chem. Soc. XXXX, XXX, XXX–XXX

(c) Murray, L. J.; Dinča, M.; Long, J. R. *Chem. Soc. Rev.* **2009**, *38*, 1294. (d) Dietzel, P. D. C.; Georgiev, P. A.; Eckert, J.; Blom, R.; Strässle, T.; Unruh, T. *Chem. Commun.* **2010**, *46*, 4962. (e) Suh, M. P.; Park, H. J.; Prasad, T. K.; Lim, D.-W. *Chem. Rev.* **2012**, *112*, 782. (f) Kapelewski, M. T.; Geier, S. J.; Hudson, M. R.; Stück, D.; Mason, J. A.; Nelson, J. N.; Xiao, D. J.; Hulvey, Z.; Gilmour, E.; FitzGerald, S. A.; Head-Gordon, M.; Brown, C. M.; Long, J. R. *J. Am. Chem. Soc.* **2014**, *136*, 12119.

(7) (a) Millward, A. R.; Yaghi, O. M. *J. Am. Chem. Soc.* **2005**, *127*, 17998. (b) Caskey, S. R.; Wong-Foy, A. G.; Matzger, A. J. *J. Am. Chem. Soc.* **2008**, *130*, 10870. (c) Bae, Y.-S.; Snurr, R. Q. *Angew. Chem., Int. Ed.* **2011**, *50*, 11586. (d) Li, J.-R.; Ma, Y.; McCarthy, M. C.; Sculley, J.; Yu, J.; Jeong, H.-K.; Balbuena, P. B.; Zhou, H.-C. *Coord. Chem. Rev.* **2011**, *255*, 1791. (e) Sumida, K.; Rogow, D. L.; Mason, J. A.; McDonald, T. M.; Bloch, E. D.; Herm, Z. R.; Bae, T.-H.; Long, J. R. *Chem. Rev.* **2012**, *112*, 724. (f) McDonald, T. M.; Mason, J. A.; Kong, X.; Bloch, E. D.; Gygi, D.; Dani, A.; Crocella, V.; Giordanino, F.; Odoh, S. O.; Drisdell, W.; Vlaisavljevich, B.; Dzubak, A. L.; Poloni, R.; Schnell, S. K.; Planas, N.; Lee, K.; Pascal, T.; Wan, L. F.; Prendergast, D.; Neaton, J. B.; Smit, B.; Kortright, J. B.; Gagliardi, L.; Bordiga, S.; Reimer, J. A.; Long, J. R. *Nature* **2015**, *519*, 303.

(8) (a) Jorgensen, W. L.; Severance, D. L. *J. Am. Chem. Soc.* **1990**, *112*, 4768. (b) Hobza, P.; Selzle, H. L.; Schlag, E. W. *J. Am. Chem. Soc.* **1994**, *116*, 3500. (c) Hobza, P.; Selzle, H. L.; Schlag, E. W. *J. Phys. Chem.* **1996**, *100*, 18790. (d) Hong, B. H.; Lee, J. Y.; Cho, S. J.; Yun, S.; Kim, K. S. *J. Org. Chem.* **1999**, *64*, 5661. (e) Tsuzuki, S.; Honda, K.; Uchimaru, T.; Mikami, M.; Tanabe, K. *J. Am. Chem. Soc.* **2002**, *124*, 104. (f) Sinnokrot, M. O.; Valeev, E. F.; Sherrill, C. D. *J. Am. Chem. Soc.* **2002**, *124*, 10887. (g) Nishio, M. *Phys. Chem. Chem. Phys.* **2011**, *13*, 13873.

(9) Kinzel, T.; Zhang, Y.; Buchwald, S. L. *J. Am. Chem. Soc.* **2010**, *132*, 14073.

(10) Lemmon, E. W., Huber, M. L.; McLinden, M. O. *NIST Standard Reference Database 23: Reference Fluid Thermodynamic and Transport Properties—REFPROP Version 8.0*; National Institute of Standards and Technology: Gaithersburg, MD, 2007.

(11) (a) Sinnokrot, M. O.; Sherrill, C. D. *J. Am. Chem. Soc.* **2004**, *126*, 7690. (b) Lee, E. C.; Hong, B. H.; Lee, J. Y.; Kim, J. C.; Kim, D.; Kim, Y.; Tarakeshwar, P.; Kim, K. W. *J. Am. Chem. Soc.* **2005**, *127*, 4530. (c) Wheeler, S. E.; Houk, K. N. *Mol. Phys.* **2009**, *107*, 749. (d) Bloom, J. W. G.; Raju, R. K.; Wheeler, S. E. *J. Chem. Theory Comput.* **2012**, *8*, 3167. (e) Hwang, J.; Li, P.; Smith, M. D.; Shimizu, K. D. *Angew. Chem., Int. Ed.* **2016**, *55*, 8086.

(12) (a) Dunitz, J. D.; Gavezzotti, A. *Angew. Chem., Int. Ed.* **2005**, *44*, 1766. (b) Forni, A.; Pieraccini, S.; Rendine, S.; Gabas, F.; Sironi, M. *ChemPhysChem* **2012**, *13*, 4224.

(13) (a) Allen, F. H. *Acta Crystallogr., Sect. B: Struct. Sci.* **2002**, *58*, 380. (b) Bruno, I. J.; Cole, J. C.; Edgington, P. R.; Kessler, M.; Macrae, C. F.; McCabe, P.; Pearson, J.; Taylor, R. *Acta Crystallogr., Sect. B: Struct. Sci.* **2002**, *58*, 389.

(14) (a) Hibbs, D. E.; Overgaard, J.; Platts, J. A.; Waller, M. P.; Hursthouse, M. B. *J. Phys. Chem. B* **2004**, *108*, 3663. (b) Bayón, R.; Coco, S.; Espinet, P. *Chem. - Eur. J.* **2005**, *11*, 1079. (c) Chopra, D.; Nagarajan, K.; Guru Row, T. N. *Cryst. Growth Des.* **2005**, *5*, 1035. (d) Matta, C. F.; Castillo, N.; Boyd, R. J. *J. Phys. Chem. A* **2005**, *109*, 3669. (e) Chopra, D.; Cameron, T. S.; Ferrara, J. D.; Guru Row, T. N. *J. Phys. Chem. A* **2006**, *110*, 10465. (f) Choudhury, A. R.; Guru Row, T. N. *CrystEngComm* **2006**, *8*, 265. (g) Mariaca, R.; Behrnd, N.-R.; Eggli, P.; Stoeckli-Evans, H.; Hulliger, J. *CrystEngComm* **2006**, *8*, 222. (h) Berger, R.; Resnati, G.; Metrangolo, P.; Weber, E.; Hulliger, J. *Chem. Soc. Rev.* **2011**, *40*, 3496. (i) Baker, R. J.; Colavita, P. E.; Murphy, D. M.; Platts, J. A.; Wallis, J. D. *J. Phys. Chem. A* **2012**, *116*, 1435.

(15) (a) Coudert, F.-X.; Jeffroy, M.; Fuchs, A. H.; Boutin, A.; Mellot-Draznieks, C. *J. Am. Chem. Soc.* **2008**, *130*, 14294. (b) Watanabe, S.; Sugiyama, H.; Adachi, H.; Tanaka, H.; Miyahara, M. *J. Chem. Phys.* **2009**, *130*, 164707. (c) Neimark, A. V.; Coudert, F.-X.; Boutin, A.; Fuchs, A. H. *J. Phys. Chem. Lett.* **2010**, *1*, 445. (d) Bousquet, D.; Coudert, F.-X.; Boutin, A. *J. Chem. Phys.* **2012**, *137*, 044118. (e) Sugiyama, H.; Watanabe, S.; Tanaka, H.; Miyahara, M. T. *Langmuir* **2012**, *28*, 5093.

(16) A description of the accessible N_2 surface area and pore volume calculations is provided in the Supporting Information.

(17) (a) International Energy Agency. *World Energy Outlook 2011: Are We Entering a Golden Age of Gas*; http://www.worldenergyoutlook.org. (b) U.S. Energy Information Administration, International Energy Statistics. *Today in Energy: Global natural gas consumption doubled from 1980 to 2010*, 2012; http://www.eia.gov. (c) Bilgen, S. *Renewable Sustainable Energy Rev.* **2014**, *38*, 890.

(18) (a) Kondo, M.; Yoshitomi, T.; Seki, K.; Matsuzaka, H.; Kitagawa, S. *Angew. Chem., Int. Ed. Engl.* **1997**, *36*, 1725. (b) Chui, S. S.-Y.; Lo, S. M.-F.; Charmant, J. P. H.; Orpen, A. G.; Williams, I. D. *Science* **1999**, *283*, 1148. (c) Noro, S.; Kitagawa, S.; Kondo, M.; Seki, K. *Angew. Chem., Int. Ed.* **2000**, *39*, 2081. (d) Ma, S.; Sun, D.; Simmons, J. M.; Collier, C. D.; Yuan, D.; Zhou, H.-C. *J. Am. Chem. Soc.* **2008**, *130*, 1012. (e) Furukawa, H.; Ko, N.; Go, Y. B.; Aratani, N.; Choi, S. B.; Choi, E.; Yazaydin, A. Ö.; Snurr, R. Q.; O'Keeffe, M.; Kim, J.; Yaghi, O. M. *Science* **2010**, *329*, 424. (f) Wilmer, C. E.; Leaf, M.; Lee, C. Y.; Farha, O. K.; Hauser, B. G.; Hupp, J. T.; Snurr, R. Q. *Nat. Chem.* **2012**, *4*, 83. (g) Peng, Y.; Krungleviciute, V.; Eryazici, I.; Hupp, J. T.; Farha, O. K.; Yildirim, T. *J. Am. Chem. Soc.* **2013**, *135*, 11887. (h) Wilmer, C. E.; Farha, O. K.; Yildirim, T.; Eryazici, I.; Krungleviciute, V.; Sarjeant, A. A.; Snurr, R. Q.; Hupp, J. T. *Energy Environ. Sci.* **2013**, *6*, 1158. (i) Gándara, F.; Furukawa, H.; Lee, S.; Yaghi, O. M. *J. Am. Chem. Soc.* **2014**, *136*, 5271. (j) He, Y.; Zhou, W.; Qian, G.; Chen, B. *Chem. Soc. Rev.* **2014**, *43*, 5657. (k) Li, B.; Wen, H.-M.; Wang, H.; Wu, H.; Tyagi, M.; Yildirim, T.; Zhou, W.; Chen, B. *J. Am. Chem. Soc.* **2014**, *136*, 6207. (l) Mason, J. A.; Veenstra, M.; Long, J. R. *Chem. Sci.* **2014**, *5*, 32. (m) Service, R. F. *Science* **2014**, *346*, 538. (n) Chang, G.; Li, B.; Wang, H.; Bao, Z.; Yildirim, T.; Yao, Z.; Xiang, S.; Zhou, W.; Chen, B. *Chem. Commun.* **2015**, *51*, 14789. (o) Song, C.; Ling, Y.; Feng, Y.; Zhou, W.; Yildirim, T.; He, Y. *Chem. Commun.* **2015**, *51*, 8508.

(19) (a) Mele, A.; Vergani, B.; Viani, F.; Meille, S. V.; Farina, A.; Bravo, P. *Eur. J. Org. Chem.* **1999**, *1999*, 187. (b) Desiraju, G. R. *Acc. Chem. Res.* **2002**, *35*, 565. (c) Parsch, J.; Engels, J. W. *J. Am. Chem. Soc.* **2002**, *124*, 5664. (d) Lee, J. H.; Kim, H. J.; Choi, Y. W.; Lee, Y. M.; Park, B. K.; Kim, C.; Kim, S.-J.; Kim, Y. *Polyhedron* **2007**, *26*, 1388. (e) O'Hagan, D. *Chem. Soc. Rev.* **2008**, *37*, 308. (f) Anzahaee, M. Y.; Watts, J. K.; Alla, N. R.; Nicholson, A. W.; Damha, M. J. *J. Am. Chem. Soc.* **2011**, *133*, 728. (g) Krackl, S.; Inoue, S.; Driess, M.; Enthaler, S. *Eur. J. Inorg. Chem.* **2011**, *2011*, 2103. (h) Prakash, G. K. S.; Wang, F.; Rahm, M.; Shen, J.; Ni, C.; Haiges, R.; Olah, G. A. *Angew. Chem., Int. Ed.* **2011**, *50*, 11761. (i) Liu, C. C.; So, L.-C.; Lo, J. C. Y.; Chan, M. C. W.; Kaneyoshi, H.; Makio, H. *Organometallics* **2012**, *31*, 5274. (j) So, L.-C.; Liu, C.-C.; Chan, M. C. W.; Lo, J. C. Y.; Sze, K.-H.; Zhu, N. *Chem. - Eur. J.* **2012**, *18*, 565. (k) Ciavardini, A.; Rondino, F.; Paladini, A.; Speranza, M.; Fornarini, S.; Satta, M.; Piccirillo, S. *Phys. Chem. Chem. Phys.* **2013**, *15*, 19360. (l) Liu, C.-C.; Chan, M. C. W. *Acc. Chem. Res.* **2015**, *48*, 1580. (m) Panini, P.; Chopra, D. In *Hydrogen Bonded Supramolecular Structures*; Li, Z., Wu, L.-Z., Eds.; Springer-Verlag: Berlin, 2015; pp 37−67.

(20) Thalladi, V. R.; Weiss, H.-C.; Bläser, D.; Boese, R.; Nangia, A.; Desiraju, G. R. *J. Am. Chem. Soc.* **1998**, *120*, 8702.

(21) (a) Wheeler, S. E.; McNeil, A. J.; Müller, P.; Swager, T. M.; Houk, K. N. *J. Am. Chem. Soc.* **2010**, *132*, 3304. (b) Wheeler, S. E. *J. Am. Chem. Soc.* **2011**, *133*, 10262. (c) Watt, M.; Hardebeck, L. K. E.; Kirkpatrick, C. C.; Lewis, M. *J. Am. Chem. Soc.* **2011**, *133*, 3854.

DOI: 10.1021/jacs.6b09155
J. Am. Chem. Soc. XXXX, XXX, XXX−XXX